Available online at www.sciencedirect.com

SciVerse ScienceDirect

Ceramics International 38 (2012) 1697–1702

CERAMICS INTERNATIONAL

www.elsevier.com/locate/ceramint

Short communication

Growth and physical properties of three-dimensional flower-like zinc oxide microcrystals

Yuan-Chang Liang

Institute of Materials Engineering, National Taiwan Ocean University, Keelung 20224, Taiwan

Received 7 July 2011; received in revised form 5 August 2011; accepted 12 August 2011
Available online 19 August 2011

Abstract

This study reports the synthesis of ZnO flower-like structures of different sizes on polycrystalline zinc foils by cathodic electrodeposition. X-ray diffraction results indicate that the obtained flower-like ZnO microcrystals had a wurtzite structure. Scanning electron microscopy images reveal that the flower-like ZnO microcrystals consisted of taper petals. The precursor concentration and electrodepositing potential had significant effects on the size of the flower-like ZnO microcrystals. An increase in precursor concentration and electrodepositing potential caused an increase in the size of the ZnO flower-like structures. The flower-like ZnO microcrystals, with an approximate petal length of 0.8–1.6 μm, exhibited a strong UV emission at room temperature, while those with a petal length of 3.0–4.2 μm produced noticeably yellow emissions.

Keywords: B. Surfaces; C. Optical properties; D. ZnO

1. Introduction

Wide bandgap semiconductor materials have attracted substantial attention because of their use in optoelectronics. Among the various wide bandgap semiconductors, ZnO is a versatile material with scientific importance because of its interesting optical, electrical, acoustic, and biocompatible properties [1,2]. Moreover, the synthesis of ZnO with various morphologies has been widely developed for various applications, such as gas sensors, varistors, solar cells, and electro- and photoluminescent devices [3–5]. To enhance the multifunctionality of ZnO, several groups recently reported that a ZnO crystal with a flower-like structure has a high surface-to-volume ratio; therefore, it is a promising medium for fabricating high-performance semiconductor devices [6,7].

Previous research investigated the synthesis of ZnO flower-like structures using wet chemical methods. For a technique to be viable for commercial applications, the growth temperature should be low enough to make it energy efficient. The wet chemical process satisfies this condition. Most ZnO flower-like structures are synthesized using the hydrothermal method [8,9]. The advantages of a high growth rate, a large area, and low cost of electrochemical deposition are promising for the preparation of ZnO crystals with various morphologies. However, research into the synthesis of ZnO flower-like structures by electrodeposition is limited [10]. The effects of process parameters on the morphology and physical properties of as-synthesized ZnO flower-like structures have not been studied thoroughly. This study reports the use of electrodeposition to form ZnO microcrystals with a flower-like structure. This study also investigates the effects of process parameters on the physical properties of the ZnO flower-like structures.

2. Experimental procedures

ZnO flower-like structures were grown by cathodic electrochemical deposition from an electrolyte containing 0.02 and 0.06 M $Zn(NO_3)_2$. Hexamethylenetetramine ($C_6H_{12}N_4$) was used as a stabilizer. The bath temperature was maintained at 90 °C during the electrodeposition of the ZnO. A standard three-electrode compartment cell was used in this experiment. Zinc foil (99.99% purity) served as the cathode. The area of the zinc foil in the electrolyte for the electrodeposition was fixed at 1 cm^2. The deposition was performed at various electrodepositing potentials from −1.6 V to −2.0 V. The as-grown samples were washed with deionized water and absolute ethanol several times before measuring the structural and physical properties.

E-mail addresses: dean1818@gmail.com, yuanvictory@gmail.cm.

0272-8842/$36.00
doi:10.1016/j.ceramint.2011.08.028

The crystal structure of the electrodeposited ZnO flower-like structures was characterized by X-ray diffraction (XRD) with Cu Kα radiation. The surface morphology of the electrodeposited ZnO flower-like structures was investigated using scanning electron microscopy (SEM). X-ray photoelectron spectroscopy (XPS) analysis of ZnO was performed to determine the film stoichiometry and chemical binding state of the constituent elements. Room temperature-dependent photoluminescence (PL) spectra were obtained using the 325 nm line of a He–Cd laser.

3. Results and discussion

Fig. 1(a)–(c) shows the morphologies of the ZnO flower-like films on zinc foil produced from a 0.02 M $Zn(NO_3)_2$ solution at various potentials. SEM images show that the ZnO flower-like architecture consisted of many tapers. The flower-like structures were well developed over the area of interest. The approximate base diameter and length of the tapers of the ZnO flower-like structures at −1.6 V were 0.4–0.8 μm and 0.8–1.6 μm, respectively. Upon increasing the potential to −1.8 V, the diameter and length of the tapers increased to 0.7–1.0 μm and 0.9–2.4 μm, respectively (Fig. 1b). The tapers reached 0.8–1.2 μm in diameter and 1.2–3.1 μm in length when the potential was increased to −2.0 V (Fig. 1c). The average diameter at the base and length of the tapers of ZnO flower-like structures increased as the deposition potential became more negative. Previous research reports a similar correlation between the size and potential for controlling ZnO electrodeposits [11]. An increase in cathodic potential caused an increase in the deposition rate, thus forming larger tapers for the ZnO flower-like structure. Fig. 1(d)–(f) shows the morphologies of the ZnO flower-like structures grown from a 0.06 M electrolyte. The approximate base diameter of the tapers of

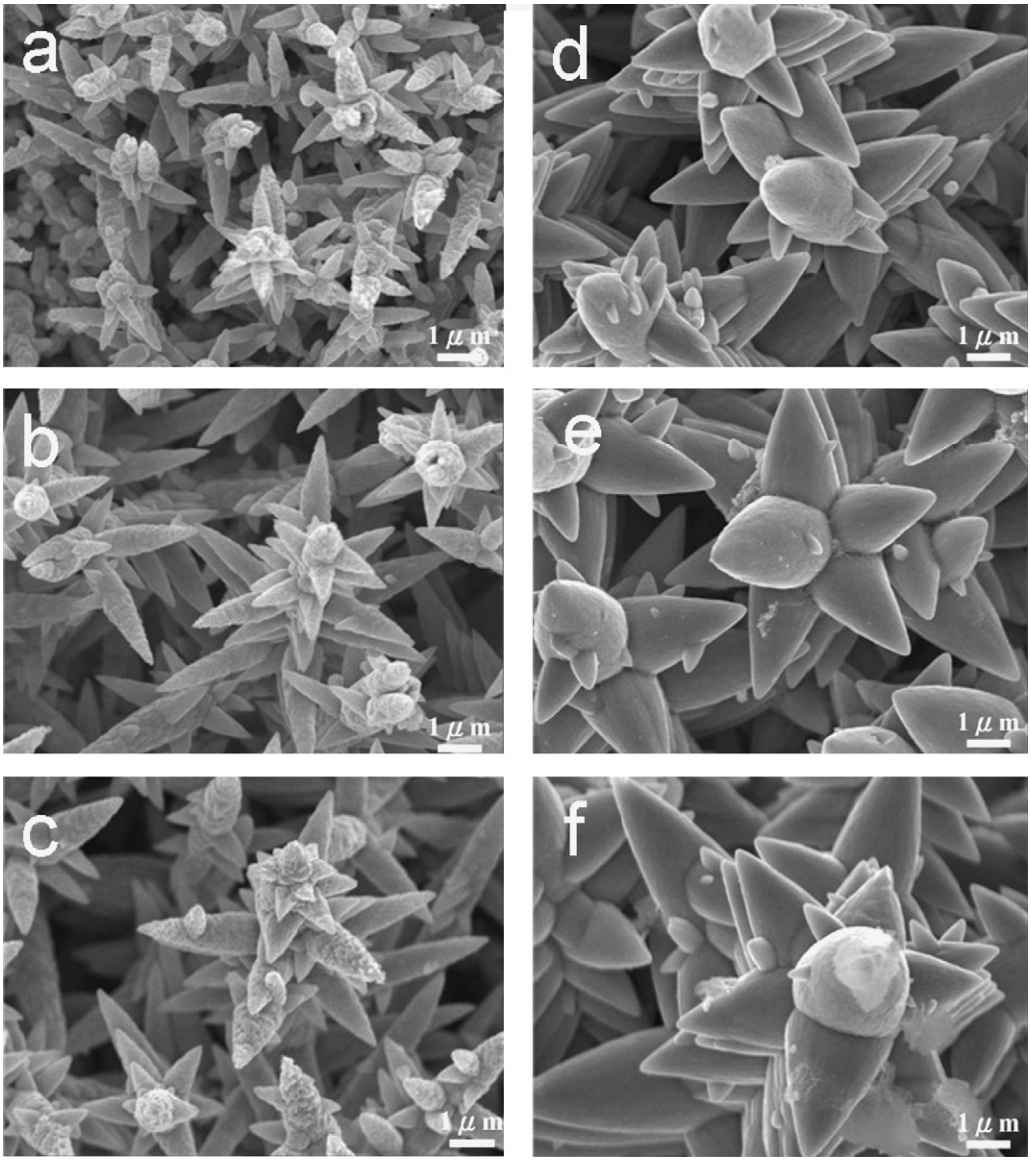

Fig. 1. SEM images of the ZnO flower-like structures grown at various process conditions: (a) 0.02 M electrolyte at −1.6 V, (b) 0.02 M electrolyte at −1.8 V, (c) 0.02 M electrolyte at −2.0 V, (d) 0.06 M electrolyte at −1.6 V, (e) 0.06 M electrolyte at −1.8 V, and (f) 0.06 M electrolyte at −2.0 V.

ZnO flower-like structures increased from 1.5–2.0 μm to 2.2–3.0 μm as the applied potential increased from −1.6 V to −2.0 V. Moreover, the length of the tapers increased from 1.7–2.2 μm to 3.0–4.2 μm when the potential reached −2.0 V. The dependence of taper size on potential is the same as that for the ZnO flower-like structures grown from the 0.02 M electrolyte. In addition to the effects of cathodic potential on the morphology of ZnO flower-like structures, a relatively dilute electrolyte results in a smaller size and height of the ZnO flower-like structures at any given potential. Previous research shows that an increase in Zn^{+} concentration might lead to faster precipitation and lower redissolution of electrodeposited ZnO [12]. The cation concentration has a significant effect on the morphology of the electrodeposited ZnO films herein.

Fig. 2 illustrates the possible growth mechanism of the ZnO flower-like structures in this study. ZnO has a number of alternating planes composed of tetrahedrally coordinated O^{2-} and Zn^{2+}, stacking alternatively along the *c*-axis. The ZnO crystal has two polar surfaces and six side facets because of its hexagonal wurtzite crystal structure (Fig. 2a). ZnO exhibits anisotropic growth, as various crystal facets have different growth rates. Kar et al. indicated that the growth rate of (0 0 1) is the fastest among all the crystallographic planes of the ZnO [13]. The growth of ZnO crystals from aqueous solutions is controlled by nucleation and growth processes. These processes are affected by the precursor concentration and the applied potentials. When the precursor concentration is high enough, ZnO nuclei will form under the applied potential. Many ZnO nuclei may aggregate together because of a reduction in the surface energy. Each nucleus in the aggregation unit subsequently grows along its *c*-axis because the polar face is thermodynamically less stable than the nonpolar faces. $Zn(OH)_4^{2-}$ has been shown to be the growth unit in $Zn(NO_3)_2$ aqueous solution, and $Zn(OH)_4^{2-}$ ions decompose to produce ZnO at a high water bath temperature [14]. The anisotropic growth of ZnO crystal involves the continuous incorporation of $Zn(OH)_4^{2-}$ from the $Zn(NO_3)_2$ electrolyte. This uneven growth results in one end of the crystal being sharp because of the diffusion-limited growth under a sufficiently high potential. The growth units facilitate the ZnO crystal growth initiating along the ⟨0 0 1⟩ direction from the six planes of hexagonal wurtzite crystal structure, resulting in a ZnO flower-like morphology. In other words, the six taper ZnO petals surround the upstanding crystal (Fig. 2b). A higher potential or higher precursor concentration causes fast nucleation, a higher degree of aggregation, and fast growth of the ZnO crystals at a given growth time. These conditions lead to the formation of a larger ZnO flower-like structure.

Fig. 3(a) and (b) displays the XRD patterns for the electrodeposited ZnO flower-like structures from various precursor concentrations and potentials. In addition to the Bragg reflections from the zinc foil substrates, the XRD patterns consist of (1 0 0), (0 0 2), (1 0 1), (1 0 2), and (1 1 0) Bragg reflections from hexagonal wurtzite ZnO. The sharp Bragg reflections confirm the formation of well-crystallized ZnO. An increase in the cathodic potential and electrolyte concentration caused an increase in the intensity of the main (0 0 2) Bragg reflection. This increase might be partially due to a significant increase in the size of the ZnO tapers with increasing cathodic potential. Moreover, the angle position of the Bragg reflections of the ZnO flower-like structures varied slightly with the applied potential. For example, Fig. 3(c) shows the magnified XRD patterns of the (0 0 2) Bragg reflections of the ZnO flower-like structures grown from a 0.06 M electrolyte. This figure clearly reveals that the Bragg reflection shifts to a lower diffraction angle as the growth potential increases. This indicates that the defect density in ZnO might increase as a

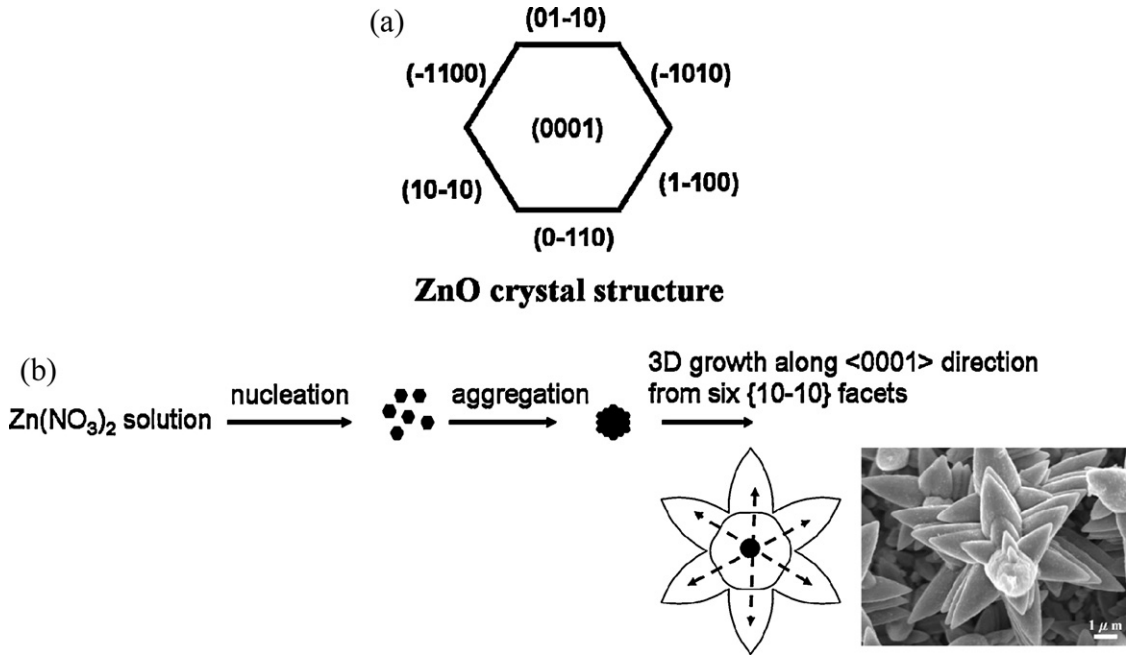

Fig. 2. Schematic illustration of the possible formation mechanism for the ZnO flower-like structure.

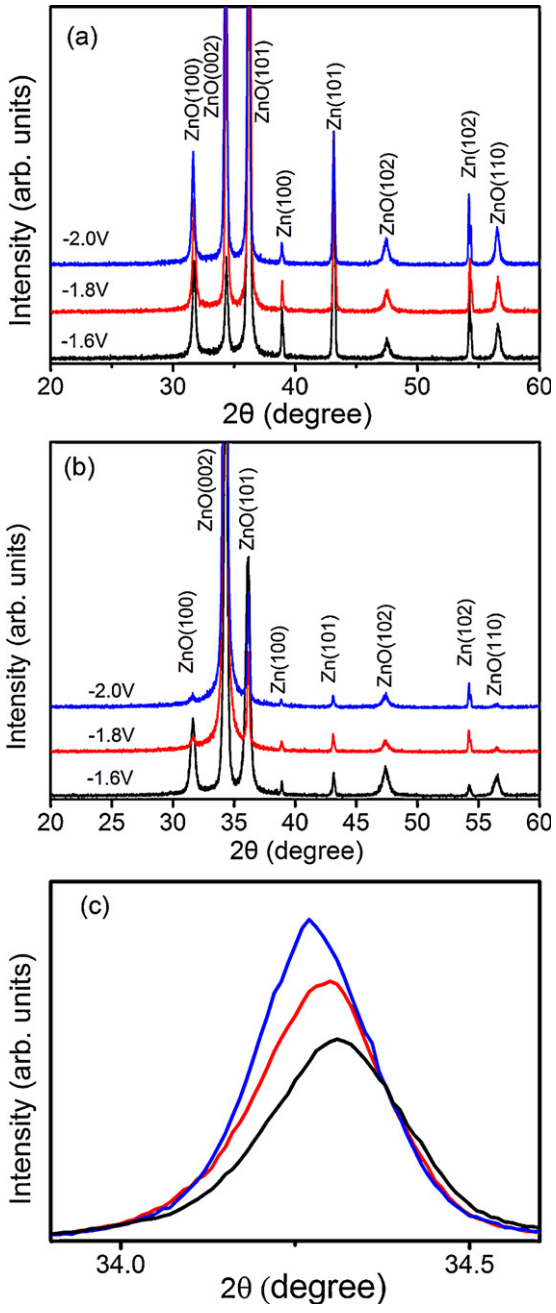

Fig. 3. XRD patterns of the ZnO flower-like structures grown from the various precursor concentrations and depositing potentials: (a) 0.02 M electrolyte, (b) 0.06 M electrolyte, and (c) the magnified XRD patterns of the (0 0 2) Bragg reflections of the ZnO flower-like structures grown from 0.06 M electrolyte at various potentials.

result of the fast growth and coalescence of the ZnO crystals at relatively high potentials.

Fig. 4 shows the representative XPS spectra for the Zn and O regions of the ZnO flower-like structures grown from a 0.02 M electrolyte at −1.8 V. The binding energies of Zn $2p_{3/2}$ and Zn $2p_{1/2}$ are 1020.9 and 1043.9 eV, respectively. These binding energies are close to the standard values of bulk ZnO [15]. The atomic ratio O/Zn calculated from the O 1s and Zn 2p peaks areas is approximately 1.16:1, which confirms the presence of a small excess of O in the ZnO flower-like structures. The O 1s

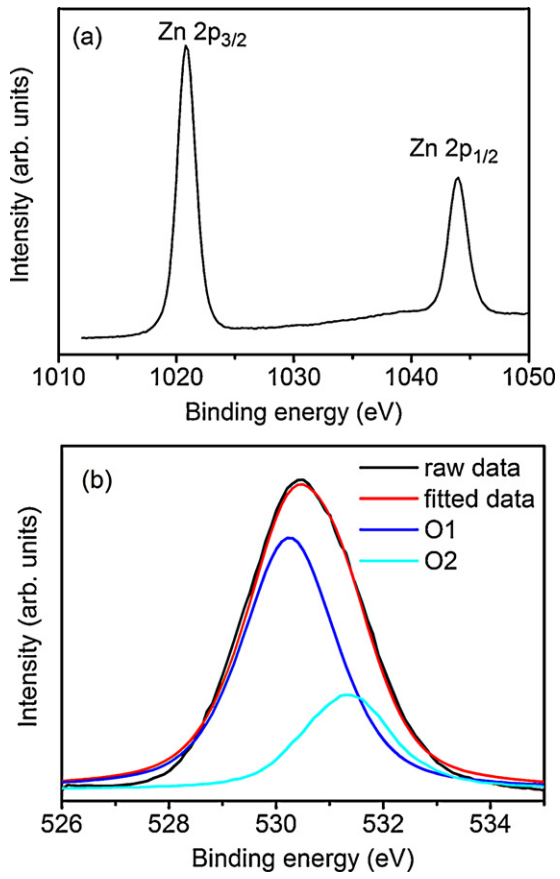

Fig. 4. Representative XPS spectra of the Zn 2p and O 1s for the ZnO flower-like structures grown from 0.02 M electrolyte at −1.8 V.

peaks were fitted by two Gaussian curves. The relatively low binding energy component (O1) at 530.24 eV is associated with the ZnO crystal lattice oxygen. The high binding energy component (O2), located at approximately 531.30 eV, suggests the presence of hydrated oxides species corresponding to OH [16]. The existence of hydrated oxide species in the ZnO flower-like structures is due to the aqueous solution process. Previous research shows similar results in ZnO films prepared from aqueous solutions [17].

Fig. 5 exhibits the PL spectra of the ZnO flower-like structures electrodeposited at various precursor concentrations and potentials. UV emission peaks were observed in all samples. This UV emission was assigned to the excitonic recombination corresponding to the band edge emission of ZnO [18,19]. In addition to the UV emission peaks, Fig. 5 shows wide yellow emission bands in the PL spectra. The source of the visible emission from ZnO is associated with defect centers. However, there is still no consensus on the origin of this yellow emission. Some researchers suggest that this yellow emission is associated with OH groups [20], while others indicate that oxygen interstitial defects are the cause for this yellow emission [21]. Fig. 5 shows that the weakening of the UV emission with the increasing potential may be ascribed to greater defects in the ZnO flower-like structures, as shown in the XRD results. A similar result has been reported for electrodeposited ZnO films on ITO substrates [22]. The presence of a stronger visible

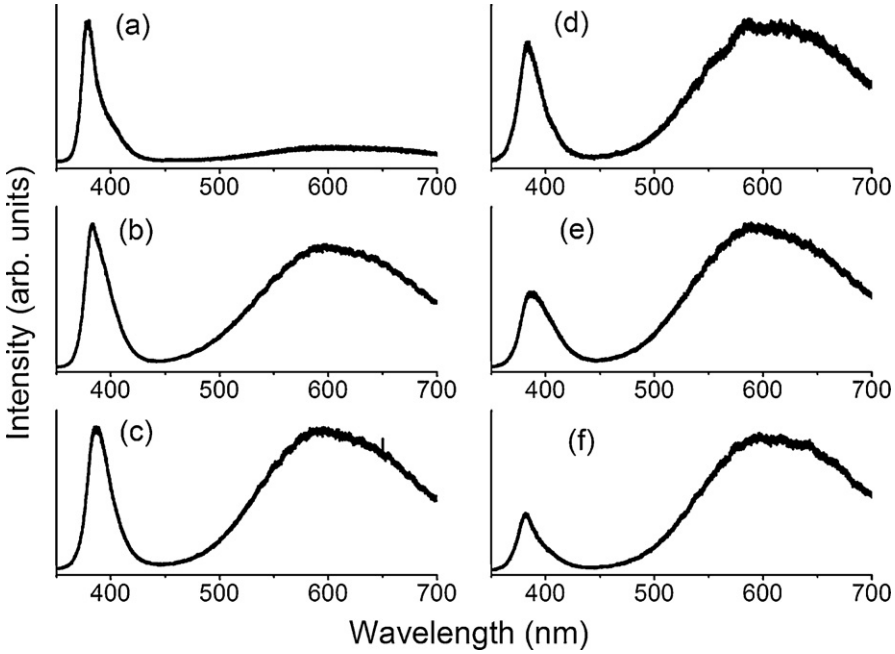

Fig. 5. PL spectra of the ZnO flower-like structures at various process conditions: (a) 0.02 M at −1.6 V, (b) 0.02 M, at −1.8 V, (c) 0.02 M at −2.0 V, (d) 0.06 M at −1.6 V, (e) 0.06 M at −1.8 V, and (f) 0.06 M at −2.0 V.

emission band in the PL spectra of electrodeposited ZnO is likely due to a fast deposition rate [23]. Moreover, a decreasing trend in the UV-to-visible emission ratio appeared as the precursor concentration increased from 0.02 to 0.06 M at a given potential. The coalescence of tapers during electrodeposition increased the defects in the ZnO crystal, yielding stronger visible emissions. An increase in precursor concentration increased the probability of coalescence of the ZnO flower-like structures, as exhibited in SEM images. This in turn created a stronger visible emission band in the PL spectra.

4. Conclusions

The synthesis of well-defined ZnO flower-like structures on polycrystalline zinc foils was realized by cathodic electrodeposition in an aqueous solution. Adjusting the precursor concentration and potential produced ZnO flower-like microcrystals of various sizes. An increase in precursor concentration and cathodic potential caused an increase in the size of the ZnO flower-like structures. The growth mechanism of the ZnO flower-like microcrystals can be described as follows: the growth units facilitated the ZnO crystal growth along the $\langle 0\,0\,1 \rangle$ direction from the six planes of the hexagonal wurtzite crystal structure during electrodeposition. The resulting flower-like ZnO microcrystals exhibited strong UV emission at a relatively low precursor concentration and potential. Using a high precursor concentration and potential produced a notable increase in the size of the flower-like ZnO microcrystals. Consequently, the ZnO microcrystals exhibited a decreasing trend in the UV-to-visible emission ratio. This might be associated with an increase in defect density in the flower-like ZnO microcrystals because of an increased rate of nucleation, aggregation, and growth at a high precursor concentration and potential.

Acknowledgements

This work was supported by the National Science Council of the Republic of China (Grant No. NSC 100-2628-E-019-003-MY2 & NSC 100-2221-E-019-059-MY2) and the National Taiwan Ocean University (Grant No. NTOU-RD-AA-2010-104031).

References

[1] K.Y. Tse, H.H. Hng, S.P. Lau, Y.G. Wang, S.F. Yu, ZnO thin films produced by filtered cathodic vacuum arc technique, Ceramics International 30 (2004) 1669–1674.
[2] K. Hirota, M. Sugimoto, M. Kato, K. Tsukagoshi, T. Tanigawa, H. Sugimoto, Preparation of zinc oxide ceramics with a sustainable antibacterial activity under dark conditions, Ceramics International 36 (2010) 497–506.
[3] J. Singh, S.S. Patil, M.A. More, D.S. Joag, R.S. Tiwari, O.N. Srivastava, Formation of aligned ZnO nanorods on self-grown ZnO template and its enhanced field emission characteristics, Applied Surface Science 256 (2010) 6157–6163.
[4] C. Ren, B. Yang, M. Wu, J. Xu, Z. Fu, Y. lv, T. Guo, Y. Zhao, C. Zhu, Synthesis of Ag/ZnO nanorods array with enhanced photocatalytic performance, Journal of Hazardous Materials 182 (2010) 123–129.
[5] W. Zhao, L. Zhao, Z. Shi, X. Xia, X. Li, X. Dong, Y. Chang, B. Zhang, G. Du, Electroluminescence of the p-ZnO:As/n-ZnO LEDs grown on ITO glass coated with GaAs interlayer, Applied Surface Science 25 (2011) 4685–4688.
[6] H. Li, Y. Ni, J. Hong, Ultrasound-assisted preparation, characterization and properties of flower-like ZnO microstructures, Scripta Materialia 60 (2009) 524–527.

[7] Y. Zhang, Y. Zhang, H. Wang, B. Yan, G. Shen, R. Yu, An enzyme immobilization platform for biosensor designs of direct electrochemistry using flower-like ZnO crystals and nano-sized gold particles, Journal of Electroanalytical Chemistry 627 (2009) 9–14.
[8] H. Zhao, X. Sua, F. Xiao, J. Wang, J. Jian, Synthesis and gas sensor properties of flower-like 3D ZnO microstructures, Materials Science and Engineering B 176 (2011) 611–615.
[9] P. Rai, J.N. Jo, I.H. Lee, Y.T. Yu, Fabrication of flower-like ZnO microstructures from ZnO nanorods and their photoluminescence properties, Materials Chemistry and Physics 124 (2010) 406–412.
[10] W. Peng, S. Qu, G. Cong, Z. Wang, Synthesis and structures of morphology-controlled zno nano- and microcrystals, Crystal Growth & Design 6 (2006) 1518–1522.
[11] Q.P. Chen, M.Z. Xue, Q.R. Sheng, Y.G. Liu, Z.F. Ma, Electrochemical growth of nanopillar zinc oxide films by applying a low concentration of zinc nitrate precursor, Electrochemical and Solid-State Letters 9 (2006) C58–C61.
[12] S. Peulon, D. Lincot, Mechanistic study of cathodic electrodeposition of zinc oxide and zinc hydroxychloride films from oxygenated aqueous zinc chloride solutions, Journal of the Electrochemical Society 145 (1998) 864–874.
[13] S. Kar, A. Dev, S. Chaudhuri, Simple solvothermal route to synthesize ZnO nanosheets, nanonails, and well-aligned nanorod arrays, Journal of Physical Chemistry B 110 (2006) 17848–17853.
[14] W.J. Li, E.W. Shi, W.Z. Zhong, Z.W. Yin, Growth mechanism and growth habit of oxide crystals, Journal of Crystal Growth 203 (1999) 186–196.
[15] J.F. Moudler, W.F. Stickle, E.P. Sobol, K.D. Bomben, Handbook of X-ray Photoelectron Spectroscopy, Perkin-Elmer, Eden Prairie, MN, 1992, pp. 52–53.
[16] S.B. Majumder, M. Jain, P.S. Dobal, R.S. Katiyar, Investigations on solution derived aluminium doped zinc oxide thin films, Materials Science and Engineering B 103 (2003) 16–25.
[17] Y.C. Liang, M.Y. Tsai, C.L. Huang, C.Y. Hu, C.S. Hwang, Structural and optical properties of electrodeposited ZnO thin films on conductive RuO_2 oxides, Journal of Alloys and Compounds 509 (2011) 3559–3565.
[18] Y.C. Liang, Growth and characterization of nonpolar *a*-plane ZnO films on perovskite oxides with thin homointerlayer, Journal of Alloys and Compounds 508 (2010) 158–161.
[19] Y.C. Liang, Growth and structural characteristics of perovskite–wurtzite oxide ceramics thin films, Ceramics International 37 (2011) 791–796.
[20] N.S. Norberg, D.R. Gamelin, Influence of surface modification on the luminescence of colloidal ZnO nanocrystals, Journal of Physical Chemistry B 109 (2005) 20810–20816.
[21] W.M. Kwok, A.B. Djurisic, Y.H. Leung, D. Li, K.H. Tam, D.L. Phillips, W.K. Chan, Influence of annealing on stimulated emission in ZnO nanorods, Applied Physics Letters 89 (2006) 183112–183114.
[22] C. Gu, J. Li, J. Lian, G. Zheng, Electrochemical synthesis and optical properties of ZnO thin film on In_2O_3:Sn (ITO)-coated glass, Applied Surface Science 253 (2007) 7011–7015.
[23] G.R. Li, X.H. Lu, D.L. Qu, C.Z. Yao, F.L. Zheng, Q. Bu, C.R. Dawa, Y.X. Tong, Electrochemical growth and control of ZnO dendritic structures, Journal of Physical Chemistry C 111 (2007) 6678–6683.